In: Hauska, H. (Ed), 1997. Proceedings ScanGIS ’97 The 6th Scandinavian research conference on GIS, 1+3 June 1997, Stockholm, pp 216-228.

PROCEEDINGS SCANGIS 1997,

Catchment-scale modelling of erosion and reservoir sedimentation

PETTER STENSTRÖM and THOMAS GUMBRICHT
Division of Land and Water Resources, Department of Civil and Environmental Engineering, KTH, S-100 44 Stockholm, Sweden.
internet: ev95_str@l.kth.se, thomgum@l.kth.se

Abstract: An index-approach to catchment-scale soil erosion modelling in six catchments in Cyprus is presented. Within a geographic information system, the four factors commonly accepted to control soil erosion processes are investigated: climate erosivity, soil erodibility, land cover and topography. The factors are combined in a compound index describing the spatial distribution of erosion susceptibility. Sensitivity to spatial resolution and quantitative errors is analysed, and the potential reservoir sedimentation is estimated via a delivery ratio.

KEYWORDS: GIS, erosion susceptibility, sediment yield, index-based modelling, topographic index, delivery ratio.

1. Introduction

Accelerated soil erosion and reservoir sedimentation are major environmental hazards in semi-arid environments (e.g. Pilesjö 1992; Tsiourtis 1993). Mitigations require that hydrologic patterns and their connections to land surface characteristics are recognized and understood. Distributed, transparent models formulated and validated at a catchment scale are needed for making links and interdependencies in the catchment distinct, and for identifying particularly susceptible areas.

Index-based models aim at predictions and characterisations of complex phenomena in heterogeneous environments. Some physical sophistication is sacrificed to allow improved representations of spatial patterns (Moore *et al.* 1993). The catchment is described in terms of a few synoptic indices, and processes occurring in the catchment are explained in terms of the spatial distribution of these indices.

The article demonstrates an approach to catchment-scale, index-based, distributed modelling of erosion and reservoir sedimentation. Within a GIS, indices on vegetation cover, rainfall erosivity, soil erodibility and topography are investigated and combined in a compound index. Data from six catchments in Cyprus is used.

In: Hauska, H. (Ed), 1997. Proceedings ScanGIS ’97 The 6th Scandinavian research conference on GIS, 1+3 June 1997, Stockholm, pp 216-228.

1.1 *Catchment-scale soil erosion modelling*

Traditionally erosion is modelled as the result of additive factors including rainfall-runoff erosivity, soil erodibility, slope length and steepness, management practices, and vegetation cover (Morgan 1986). Physical models based on continuum assumptions and on the laws of mass and energy conservation have led to rigorous mathematical descriptions of coupled water, weathering and erosion processes. Simplifications have been introduced for building distributed field erosion models. Empirical models are more common, with the linear, multiplicative Universal Soil Loss Equation (USLE, Wischmeier and Smith 1978) and its derivatives by far being the most widely used. The models are distributed and data hungry. Thus remote sensing and GIS are now widely adopted for parameter estimation in both physical and empirical models (Wilson 1997). Notably applications of empirical models in developing countries rely heavily on GIS and remote sensing for parameter estimation (e.g. Pilesjö 1992; Chenevey 1995). Recently elaborated physically-based erosion models have been fully integrated with GIS (De Roo *et al.* 1996). However, the success of both physical and empirical cause-effect modelling is increasingly questioned (e.g. Beven 1989; Gumbricht 1996). A development in environmental modelling has thus been towards a holistic index approach which includes the key factors determining system behaviour, but is based on simplified representations of the underlying physics.

The distribution of erosion potential in a catchment is strongly related to the distribution and characteristics of the drainage network. Accurate elevation models (e.g. Hutchinson 1989; Mitasova *et al.* 1995), adequate flow routing algorithms (e.g. Quinn *et al.* 1991) and representative topographic indices (e.g. Moore *et al.* 1991) are thus prerequisites for catchment-scale erosion models. The USLE represents topography through the Length-Slope (LS) factor, written as:

$$LS=(L/22.13)^{m}*(65.4*\sin^{2}ß+4.56*\sinß+0.0065) \qquad \text{(Equation 1)}$$

where L=slope length [m], ß=slope angle [deg] and m is a constant. The relationships expressed by the equation were derived from data obtained on croplands on slopes ranging from 2 to 10 degrees in steepness and 10 to 100 meters in length. Little has been done to validate the equation outside these ranges. Moreover, slope length is a one dimensional attribute that cannot handle converging or diverging flow. These are perhaps not severe shortcomings on plane or nearly plane farm fields, but can be expected to gain significance in complex terrain. Moore and Burch (1986) derived a sediment transport capacity index (T) from unit stream power theory, which was shown to be consistent with the LS factor within the ranges of the latter if written as:

$$T=(A_s/22.13)^{0.4}*(\sinß/0.0896)^{1.3} \qquad \text{(Equation 2)}$$

In: Hauska, H. (Ed), 1997. Proceedings ScanGIS ’97 The 6th Scandinavian research conference on GIS, 1+3 June 1997, Stockholm, pp 216-228.

where A_S=specific catchment area [m^2m^{-1}] and ß=slope angle [deg]. This physically-based index should be more appropriate in complex terrain, since it explicitly accounts for flow convergence and divergence through the A_S term (Wilson 1997). Mitasova *et al*. (1995) compared T and LS in a small catchment and found that T gave more realistic distributions of topographic potential for erosion.

A particular problem in catchment-scale soil movement assessment, and in the estimation of catchment sediment yield, is to separate erosion areas from deposition areas (e.g. Wilson 1997). Hession and Shanholtz (1988) used a delivery ratio,

$$DR=const.*(h/l) \quad \text{(Equation 3)}$$

where h is the height difference between a given cell and the associated stream cell, and l is the distance. This ratio cannot identify the actual locations of deposition areas, but accounts for the higher proportion deposition areas in large flat catchments as compared to smaller and steeper catchments.

2. Study site - Cyprus

Cyprus is the third largest island in the Mediterranean sea. It is situated close to the Asian landmass and has therefore a climate that is hotter and dryer than the average Mediterranean. Summers last from April to October and are hot with barely no rain. The mean annual precipitation ranges from 1100 mm in the mountainous parts to 200 mm in the eastern plains, and averages about 500 mm (Hessling 1995). The pronounced seasonal pattern where long dry periods are followed by heavy rains in the beginning of the wet season, in combination with intense agricultural activity, makes the landscape highly susceptible to erosion.

The geology can be broadly divided into four east-west trending features: the Kyrenia range in the north, consisting of limestones and marbles and reaching heights up to 900 meters; the basaltic Troodos massif in the centre, with the highest peak at 1952 meters; the Mesaoria sedimentary plain in-between; and the Mammonia sandstone complex south of Troodos (Mahlander and McCarthy 1995). Forests are found in the Troodos mountains at elevations above 1200 m. The plains are sparsely covered or heavily cultivated (Tsiourtis 1993).

Six catchments were studied: Pomos and Argaka on the northern slopes of Troodos; Mavrokolymbos on the Mammonia complex; Polemidhia and Yermasoyia on the south-eastern slopes of Troodos; and Kiti on the Mesaoria plain (figure 1).

In: Hauska, H. (Ed), 1997. Proceedings ScanGIS '97 The 6th Scandinavian research conference on GIS, 1+3 June 1997, Stockholm, pp 216-228.

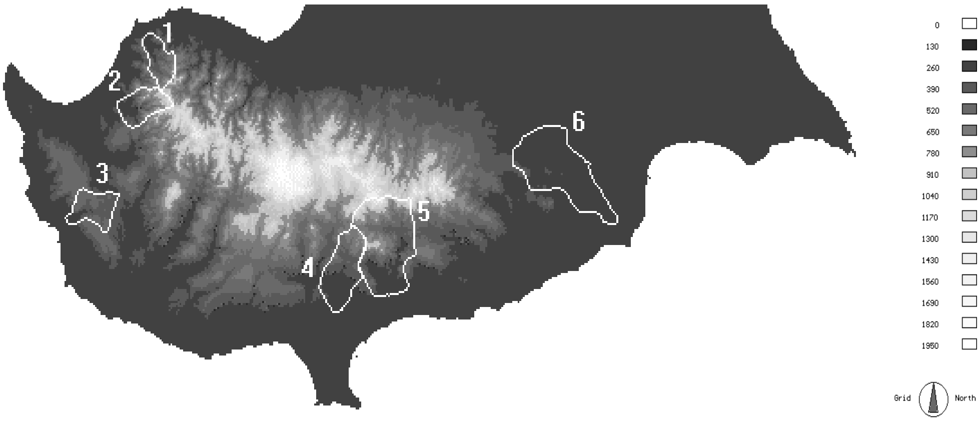

Figure 1. The studied catchments outlined on an elevation model. The northern parts with the Kyrenia range are missing. 1=Pomos, 2=Argaka, 3=Mavrokolymbos, 4=Polemidhia, 5=Yermasoyia, 6=Kiti.

3. **Materials and methods**

Two raster-based GIS, IDRISI4.1 and GRASS4.1 were used. The program USLE2D2.2 (Desmet 1994; Desmet and Govers 1994) was used for calculation of the LS factor.

A standard corrected Landsat MSS image recorded in April 1987 was used for the construction of the vegetation index. The nominal ground resolution 79 m was resampled to 50 m. Vegetation density was calculated as leaf area index (LAI) as given in McCarthy (1996).

A DEM interpolated to 50 m resolution from digitized contours with the equidistance 100 m (map scale = 1: 50 000) was used for derivation of topographic indices. Three areas of 1 km^2 size each were digitised from topographic maps in the scale 1: 5000 and used for interpolation of 10 m resolution DEMs, also resampled to 50 meter and used as ground truth when estimating the error of the former 50 m DEM.

A map with iso-contours of rainfall erosivity was available from previous soil loss studies (Michaelides and Krone 1994). In addition, time series of precipitation from 30 stations were available. Digital soil and geological images with the resolution 300 m were used. The soil image had classes according to FAO/UNESCO (1973).

The expert system GUIDE (Gumbricht 1996) was used to infer knowledge in the erosion susceptibility classification. Input rules are of the form "if condition 1, (and condition 2, and...) then conclusion". Conditions have the form of operators (=x, <x, >x, <x<). The conclusion is true if all conditions are true. GUIDE outputs a raster map with the pixel values representing the application of the rules.

In: Hauska, H. (Ed), 1997. Proceedings ScanGIS '97 The 6th Scandinavian research conference on GIS, 1+3 June 1997, Stockholm, pp 216-228.

4. Results

Comparison between the two 50 m DEMs revealed a normally distributed error with a mean close to zero and a standard deviation around 35 m. This error was randomly draped over the finer resolution (correct) DEM so that the error of this image equalled these estimates. To create a spatial correlation of the error, the image was filtered with a 3x3 mean filter. Visual inspection of the filtered image and the original image of the difference between the two DEMs had a pattern similarity, and the filtered error image was accepted.

Specific catchment areas were derived from the three areas with 10 m DEMs, and the sediment transport capacity index was calculated with equation 2 (figure 2a). It was not possible to get realistic distributions of the specific catchment area from the 50 m DEM, why the LS factor was used instead. The LS factor was derived from the 10 m DEMs, from the original (coarser) 50 m DEM, and from the 50 m DEM with the error added (figure 2). The three LS factors show similar distributions, whereas the transport capacity index appears very different (figure 2b). The two LS factors derived from the 50 m DEMs were used in the final classification.

The precipitation data from the 30 stations were found to be well correlated (R2=0.7) with elevation, longitude and latitude. A regression formula was derived and used for construction of a raster image of mean annual precipitation. The image showed distributions similar to those of the rainfall erosivity image from Michaelides and Krone (1994), and the latter was thus used in the final classification (figure 3).

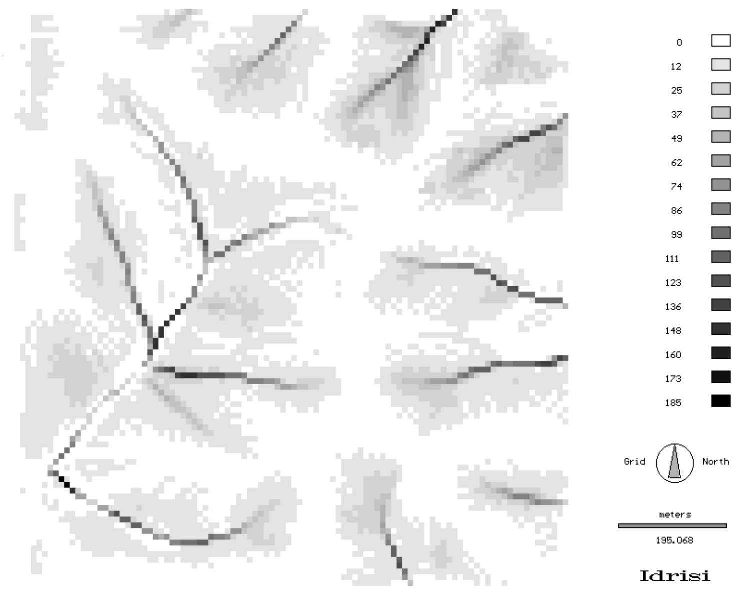

Figure 2*a*. Sediment transport capacity (estimated as T) in a small 1 km^2 part of the Yermasoyia catchment.

In: Hauska, H. (Ed), 1997. Proceedings ScanGIS '97 The 6th Scandinavian research conference on GIS, 1+3 June 1997, Stockholm, pp 216-228.

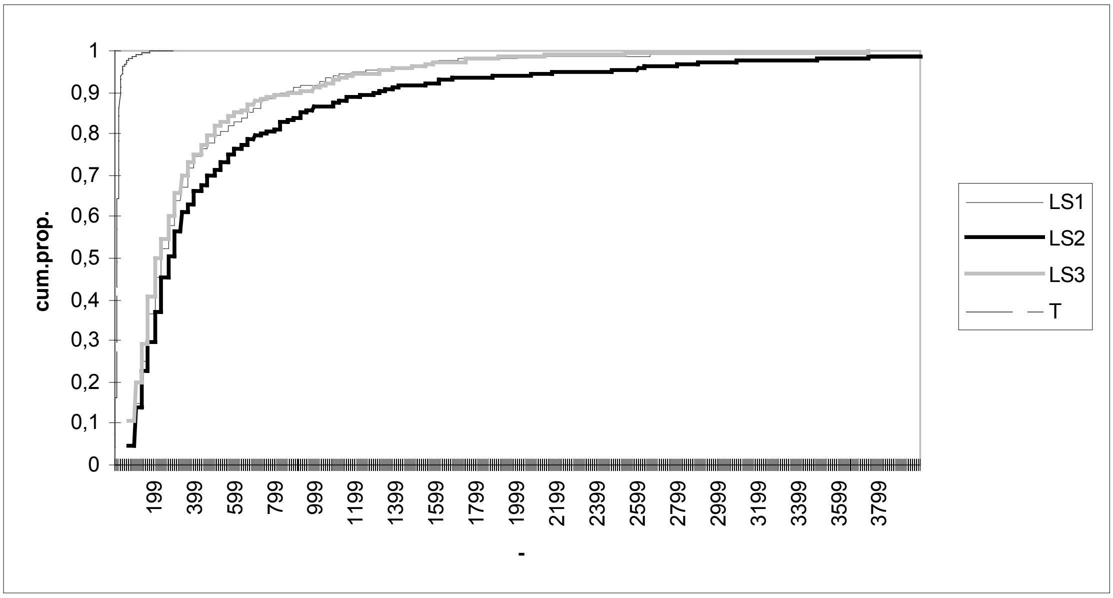

Figure 2*b*. Topographic indices from different DEMs. LS1 and T are derived from the 10 m DEM in figure 2*a*. LS2 is derived from the original 50 m DEM and LS3 from the 50 m DEM with the error added, both covering the same area as in figure 2*a*.

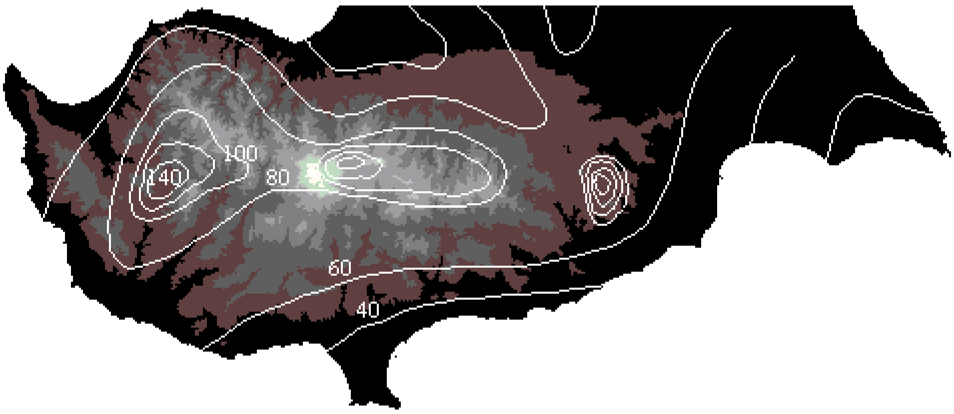

Figure 3. Rainfall erosivity contours (from Michaelides and Krone 1994) superimposed on the DEM.

The soil image was divided into two classes, where the first class (the most erodible) included immature soils (indicating mass movements), and the second soils with some structural development or soils with high organic content. The geological map was also divided into two classes were the first class (the most erodible) included sedimentary formations, and the second igneous rocks.

In: Hauska, H. (Ed), 1997. Proceedings ScanGIS '97 The 6th Scandinavian research conference on GIS, 1+3 June 1997, Stockholm, pp 216-228.

Erosion susceptibility was qualitatively classified in eight classes. Rules for the classification were written and used as input to GUIDE (appendix 1). GUIDE was run two times for each catchment, first with the LS factor from the original 50 m DEM, and then with the LS factor from the 50 m DEM with the error added. The classification showed not to be very sensitive to the differences in the LS factors (table 1). The output from the first classification is shown in figure 4.
Sediment delivery ratio images were constructed with equation 3, with the constant set to unity. The images were multiplied with the erosion susceptibility images, and the pixel values were summed for each product image to give lumped relative measures of catchment sediment yield, i.e. of potential reservoir sedimentation (figure 5).

Table 1. Comparison between erosion susceptibility classifications (mean/standard deviation)

	LS from original DEM	LS from DEM with error added
Pomos	**3.9/2.1**	**4.0/2.2**
Argaka	**3.6/2.2**	**3.7/2.3**
Mavrokolymbos	**4.4/2.4**	**4.2/2.2**
Polemidhia	**4.8/2.1**	**4.7/2.0**
Yermasoyia	**4.8/2.2**	**4.6/2.1**
Kiti	**4.5/2.6**	**4.3/2.4**

In: Hauska, H. (Ed), 1997. Proceedings ScanGIS ’97 The 6th Scandinavian research conference on GIS, 1+3 June 1997, Stockholm, pp 216-228.

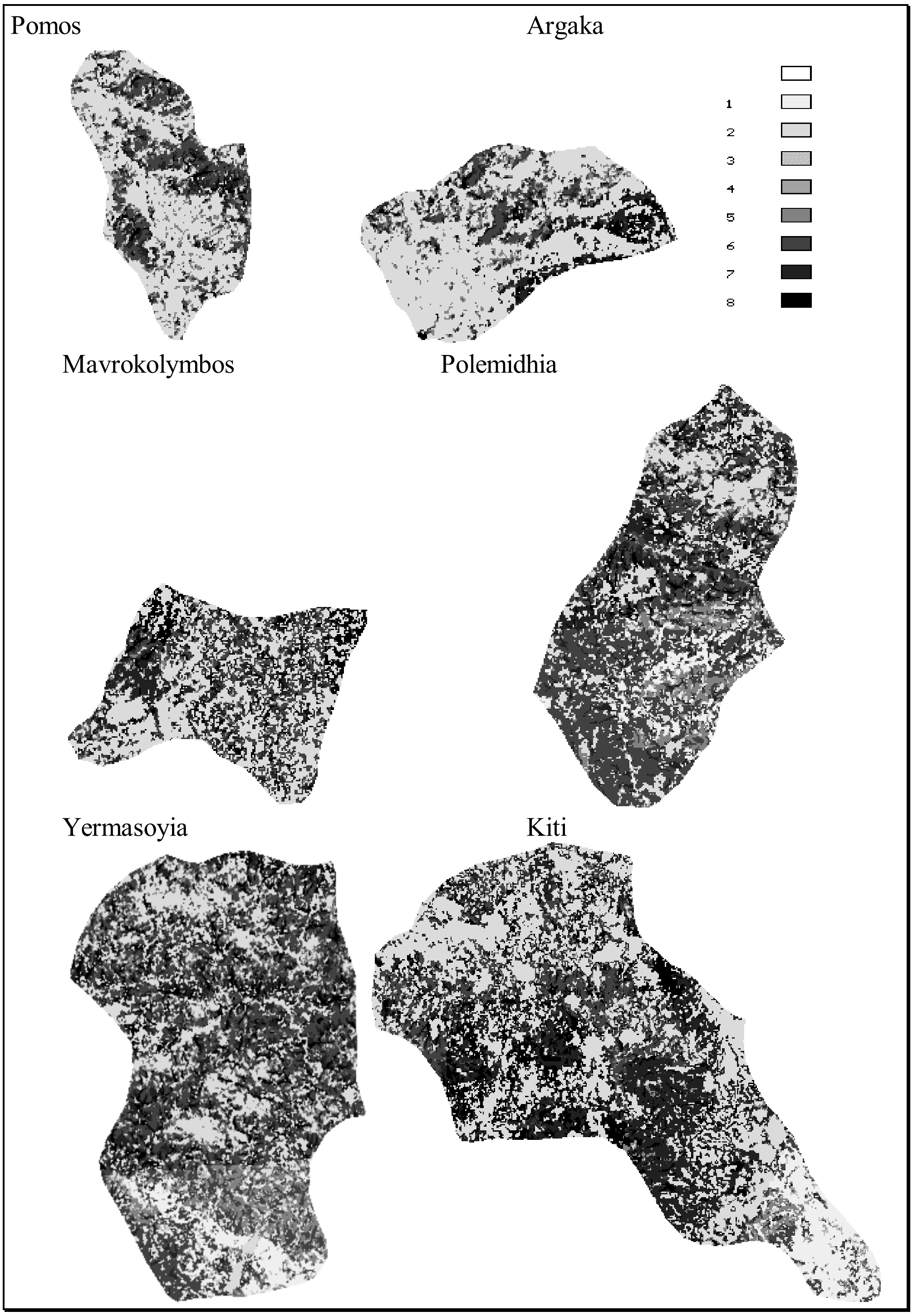

Figure 4. Erosion susceptibility in eight classes, pixels in class eight are most susceptible.

In: Hauska, H. (Ed), 1997. Proceedings ScanGIS '97 The 6th Scandinavian research conference on GIS, 1+3 June 1997, Stockholm, pp 216-228.

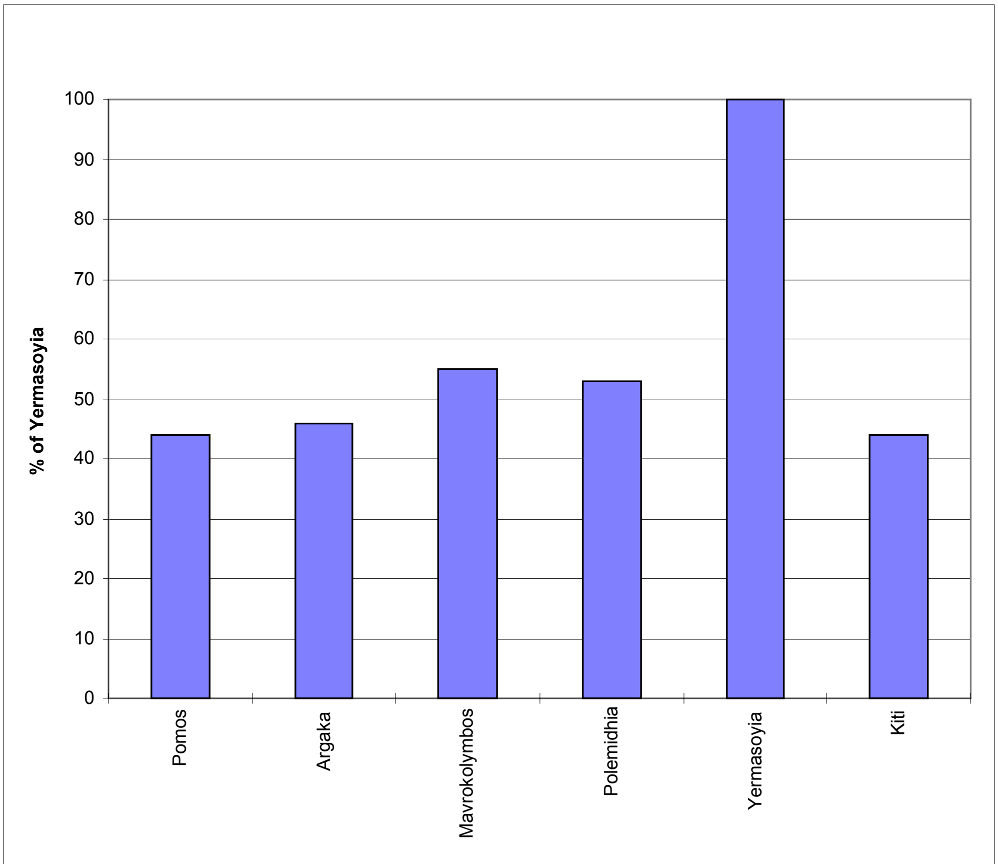

Figure 5. Catchment sediment yield, percent of the largest yield (Yermasoyia catchment)

5. Discussion and Conclusions

The presented model shows broad trends in the studied processes. It may do for a rough comparison of different catchments and sub-catchments concerning erosion susceptibility and sediment yield. Pomos and Argaka situated on the northern slopes of Troodos, on igneous rock and with a relatively high proportion forests, have the lowest average erosion susceptibility. Polemidhia on the Mammonia complex and Yermosoyia on the south-eastern slopes of Troodos, both on sedimentary formations, with sparse land cover and with a high mean slope, have the highest average susceptibility. Kiti on the Mesaoria plain and Mavrokolymbos on the Mammonia formations have intermediate average susceptibilities.

For more detailed and more reliable trends, a better data set is needed. Most crucial is an accurate DEM with sufficient resolution, and temporally resolved land cover data. Training data are required for calibration of both the susceptibility model and the delivery ratio. The susceptibility rules have to be checked for specification errors, i.e. it has to be checked if the classification is too biased towards any of the indices. If accurate quantitative measures are needed, the model has to be developed within extensive field monitoring programs. The relative importance of different erosion processes, and the magnitude and frequency of single, catastrophic events, have to be examined. However, the proposed model structure allows important spatial and temporal patterns to be reproduced, and has a satisfactory transparency. The separation of rules and data facilitates evaluation of different hypotheses, and restatement as knowledge is gained and ideas change.

Acknowledgements:

Data were supplied by The Cyprus Ministry of Agriculture, Natural Resources and Environment, Nicosia, Cyprus. We specially thank Dr Panayiotou, Mr Iacovides and the personnel at the Water Development Department, the personnel at the Remote Sensing Centre, and Mr Michaelides and Mr Markides at the Land Use Section. Thanks also to Jenny McCarthy, Martin Hessling, Camilla Mahlander and Hans Hauska at the Royal Institute of Technology.

APPENDIX 1 Rules for erosion susceptibility classification

```
WHENIMG < 13  lai
ALSOIMG < 60  rain
ALSOIMG < 300 ls
ALSOIMG = 1 geo
ALSOIMG = 2 soil
SAVEIMG # 5 class 5
!
WHENIMG < 13 lai
ALSOIMG < 60 rain
ALSOIMG < 300 ls
ALSOIMG = 2 geo
SAVEIMG # 5 class 5
!
WHENIMG < 13 lai
ALSOIMG < 60 rain
ALSOIMG > 900 ls
ALSOIMG = 1 geo
SAVEIMG # 7 class 7
!
WHENIMG < 13 lai
ALSOIMG < 60 rain
SAVEIMG # 6 class 6
!
WHENIMG < 13 lai
ALSOIMG @ 60 TO 90 rain
ALSOIMG < 300 ls
ALSOIMG = 2 soil
ALSOIMG = 1 geo
SAVEIMG # 6 class 6
!
WHENIMG < 13 lai
ALSOIMG @ 60 TO 90 rain
ALSOIMG < 300 ls
ALSOIMG = 2 geo
SAVEIMG # 6 class 6
!
WHENIMG < 13 lai
ALSOIMG @ 60 TO 90 rain
ALSOIMG < 900 ls
SAVEIMG # 7 class 7
!
WHENIMG < 13 lai
ALSOIMG > 90 rain
ALSOIMG < 300 ls
ALSOIMG = 2 geo
SAVEIMG # 7 class 7
!
WHENIMG < 13 lai
SAVEIMG # 8 class 8
!
WHENIMG @ 13 TO 16 lai
ALSOIMG < 60 rain
ALSOIMG < 300 ls
SAVEIMG # 3 class 3
!
WHENIMG @ 13 TO 16 lai
ALSOIMG < 60 rain
ALSOIMG @ 300 TO 900 ls
ALSOIMG = 2 soil
ALSOIMG = 2 geo
SAVEIMG # 3 class 3
!
WHENIMG @ 13 TO 16 lai
ALSOIMG < 60 rain
ALSOIMG < 900 ls
SAVEIMG # 4 class 4
!
WHENIMG @ 13 TO 16 lai
ALSOIMG @ 60 TO 90 rain
ALSOIMG @ 300 TO 900 ls
ALSOIMG = 1 geo
SAVEIMG # 6 class 6
!
WHENIMG @ 13 TO 16 lai
ALSOIMG @ 60 TO 90 rain
ALSOIMG > 900 ls
ALSOIMG = 2 geo
SAVEIMG # 6 class 6
!
WHENIMG @ 13 TO 16 lai
ALSOIMG @ 60 TO 90 rain
ALSOIMG > 900 ls
SAVEIMG # 7 class 7
!
WHENIMG @ 13 TO 16 lai
ALSOIMG < 90 rain
SAVEIMG # 5 class 5
!
WHENIMG @ 13 TO 16 lai
ALSOIMG > 90 rain
ALSOIMG < 300 ls
ALSOIMG = 2 soil
ALSOIMG = 1 geo
SAVEIMG # 6 class 6
WHENIMG @ 13 TO 16 lai
ALSOIMG > 90 rain
ALSOIMG < 300 ls
ALSOIMG = 2 geo
SAVEIMG # 6 class 6
!
WHENIMG @ 13 TO 16 lai
ALSOIMG > 90 rain
SAVEIMG # 7 class 7
!
WHENIMG > 16 lai
ALSOIMG < 60 rain
SAVEIMG # 1 class 1
!
WHENIMG > 16 lai
ALSOIMG < 90 rain
ALSOIMG < 300 ls
SAVEIMG # 1 class 1
!
WHENIMG > 16 lai
ALSOIMG < 90 rain
ALSOIMG < 900 ls
ALSOIMG = 2 soil
ALSOIMG = 1 geo
SAVEIMG # 2 class 2
!
WHENIMG > 16 lai
ALSOIMG < 90 rain
ALSOIMG < 900 ls
ALSOIMG = 2 geo
SAVEIMG # 2 class 2
!
WHENIMG > 16 lai
ALSOIMG < 300 ls
SAVEIMG # 2 class 2
!
WHENIMG > 16 lai
SAVEIMG # 3 class 3
```

In: Hauska, H. (Ed), 1997. Proceedings ScanGIS '97 The 6th Scandinavian research conference on GIS, 1+3 June 1997, Stockholm, pp 216-228.

References

BEVEN, K., 1989, Changing ideas in hydrology - the case of physically-based models, *Journal of Hydrology*, **105**, 157-172.

CHENEVEY, R., 1995, Hydrological modelling and erosion potential. A GIS and remote sensing approach. Royal Institute of Technology, Div. of Hydraulic Engineering. TRITA-VBI-166. Dissertation, Stockholm.

DE ROO, A.P.J., WESSELING, C.G., JETTEN, V.G. and RITSEMA, C.J., 1996, LISEM: a physically-based hydrological and soil erosion model incorporated in a GIS. In *Application of GIS in hydrology and water resources management*, edited by K. Kovar and P. Nachtnebel, IAHS Publ. No 235, pp. 395-403.

DESMET, P.J.J., 1994, USLE2D.EXE (release 2.2) user documentation. Labaratory for Experimental Geomorphology, Katholieke Universitet, Leuven, Belgium.

DESMET, P.J.J. and GOVERS, G., 1994. Potentials of a GIS-based, three-dimensional USLE-approach for the identification of critical areas at at the catchment-scale. Working paper USLE-1. Labaratory for Experimental Geomorphology, Katholieke Universitet, Leuven, Belgium.

FAO/UNESCO, 1973, Soil map of the world. Soil Resources Development and Conservation Services, Land and Water Development Division, FAO, Rome.

GUMBRICHT, T., 1996, Modelling water and vegetation reciprocity- a landscape synthesis in GIS. Division of Land and Water Resources, Department of Civil and Environmental Engineering, Royal Institute of Technology, Dissertation, Stockholm.

HESSLING, M., 1995, Water cycle modelling integrating landscape pattern- a case study in Cyprus. Master of Science degree project, Division of Land and Water Resources, Department of Civil and Environmental Engineering, Royal Institute of Technology, Stockholm.

HESSION, W.C. and SHANHOLTZ, V.O., 1988, A geographic information system for targeting nonpointsource agricultural pollution. *Journal of Soil and Water Conservation*, May-June, 264-266.

HUTCHINSON, M.F., 1989, A new procedure for gridding elevation and stream line data with automatic removal of spurious pits. *Journal of Hydrology*, **106**, 211-232.

MAHLANDER, C. and MCCARTHY J., 1995, Digital interpretation and management of land cover- a case study in Cyprus. Master of Science degree project, Division of Land and Water Resources, Department of Civil and Environmental Engineering, Royal Institute of Technology, Stockholm.

MCCARTHY, J., 1996, Leaf area index for hydroclimatological models. In *proceedings Nordic Hydrological Conference*, edited by O. Sigurdsson, K. Einarsson and H. Adalsteinsson, NHP-Report No. 40, pp. 205-214.

MICHAELIDES, PH. and KRONE, F., 1994, The effect of crop cover and management practices on soil erosion losses and grain yield. Results of long-term erosion

In: Hauska, H. (Ed), 1997. Proceedings ScanGIS ’97 The 6th Scandinavian research conference on GIS, 1+3 June 1997, Stockholm, pp 216-228.

measurements in Cyprus. Federal Institute for Geosciences and Natural Resources, Hannover.

MITASOVA, H., HOFIERKA, J., ZLOCHA, M. and IVERSON, L.R., 1995, Modeling topographic potential for erosion and deposition using GIS. *International Journal of Geographical Information Systems*, 1/16/95.

MOORE, I.D. and BURCH, G.J., 1986, Physical basis of the length-slope factor in the Universal Soil Loss Equation. *Soil Science Society of America Journal*, **50**, 1294-1298.

MOORE, I.D., GRAYSON, R.B. and LADSON, A.R., 1991, Digital terrain modelling: a review of hydrological, geomorphological and biological applications. *Hydrological Processes*, **5**, 3-30.

MOORE, I.D., TURNER, A.K., WILSON, J.P., JENSON, S.K. and BAND, L.E. (1993). GIS and land-surface-subsurface process modelling. In *Environmental modelling with GIS*, edited by M.F. Goodchild, B.O. Bradley and L.T., Steyart, Oxford University Press, pp. 196-230.

MORGAN, R.P.C., 1986, Soil Erosion & Conservation. Longman, Essex, UK.

PILESJÖ, P., 1992, GIS and Remote Sensing for Soil Erosion Studies in Semi-arid Environments. Estimation of soil erosion parameters at different scales. Dissertation, Lund University Press, Sweden.

QUINN, P., BEVEN, K., CHEVALLIER, P. and PLANCHON, O., 1991, The prediction of hillslope flow paths for distributed hydrological modelling using digital terrain models. *Hydrological processes*, **5**, 59-79.

TSIOURTIS, N., 1993, Reservoir sedimentation and its control in Cyprus. Water Development Department, Ministry of Agriculture and Natural Resources, Nicosia.

WILSON, J.P., 1997, Spatial models of land use systems and soil erosion: The role of GIS. In *Spatial models and GIS: new potential for new models*?, edited by S. Fotheringham and M. Wegener. In press.

WISCHMEIER, W.H. and SMITH, D.D., 1978, Predicting Rainfall Erosion Losses. Agricultural Handbook, US Dept. of Agriculture, Washington D.C.

In: Hauska, H. (Ed), 1997. Proceedings ScanGIS '97 The 6th Scandinavian research conference on GIS, 1+3 June 1997, Stockholm, pp 216-228.